The 2025 World Congress on
Advances in Structural Engineering and Mechanics (ASEM25)
BEXCO, Busan, Korea, August 11-14, 2025

Monitoring Sinkhole Deformation with WT-SBAS-InSAR

*Naeryoung Choi[1)], Lang Fu[2)], Inyoung Lee[3)], Hyungjoon Seo[4)]

[1), 3), 4)] *Department of Civil Engineering, Seoul National University of Science and Technology, SEOUL, 01811, Korea*
[2)] *Department of Civil and Environmental Engineering, University of Liverpool, UK L69 7ZX, UK*
[1)] *sofud791@seoultech.ac.kr* [2)] *L.Fu8@Liverpool.ac.uk* [3)] *liy5984@seoultech.ac.kr*
[4)]*hjseo@seoultech.ac.kr*

ABSTRACT

With the increasing frequency of sinkhole occurrences in urban areas, accurate monitoring is increasingly important. This study aims to analyze the ground behavior around two sinkhole sites in Seoul. Sentinel-1 C-band satellite data were utilized to collect ground displacement information from 2018 to 2025, and SBAS-InSAR techniques were applied to analyze long-term subsidence trends. For each sinkhole site, InSAR data from nearby points of the sinkholes and points located at a certain distance away from the sinkholes were compared. In this study, an analysis method, which is called WT-SBAS-InSAR Analysis, for detecting sinkhole was developed. The wavelet transform analysis was performed on the raw data of InSAR to visually detect abnormal ground deformation patterns. As a result, while the raw data of InSAR itself did not clearly reveal sinkhole occurrences, the Wavelet Transform analysis successfully detected increases in frequency values around the time of the sinkhole events. In contrast, points located far from the sinkholes did not show any significant deformation. This study demonstrates the potential of satellite-based techniques for detecting ground behavior related to sinkhole occurrences and suggests that, when combined with machine learning approaches, these methods could contribute to improved urban infrastructure safety through predictive modeling.

Keywords: SBAS-InSAR; Wavelet Transform Analysis; Sinkhole Early Warning; Time–Frequency Signal Analysis; Urban Ground Stability Monitoring

1. INTRODUCTION

[1), 3)] Undergraduate Student
[2)] Ph.D. Student
[4)] Professor

Sinkholes are one of the most prominent hazards in karst regions, where the collapse of subsurface cavities often leads to sudden ground failures. These features pose significant threats to urban and suburban infrastructure, causing severe damage and triggering secondary risks (Dobecki and Upchurch, 2006; Gutiérrez et al., 2014). In the United States alone, sinkhole-related losses are estimated to exceed $300 million annually (Weary, 2015). While natural karstic processes are a primary cause, urban sinkholes are also frequently linked to anthropogenic factors such as leaking underground pipelines and inefficient stormwater drainage, which accelerate subsurface erosion (Kaufmann and Quinif, 2002; Van Den Eeckhaut et al., 2007).

The identification and monitoring of sinkholes remain challenging due to their hidden and often abrupt formation processes. Although techniques such as GPR, ERT, and shallow seismic surveys are commonly employed (Theron and Engelbrecht, 2018; Carbonel et al., 2014), they are often expensive and labor-intensive, and are typically conducted after visible signs of deformation have appeared (Engelbrecht et al., 2011). Previous studies have highlighted the potential of remote sensing technologies such as LiDAR and SAR for detecting ground deformation with improved spatial and temporal resolution (Becker et al., 2024; Seo et al., 2022; Krieger et al., 2013).

InSAR technology has been widely used in monitoring research on the spatial and temporal evolution of sinkholes in many locations. For example, it has been successfully used to monitor sinkhole activities in the Dead Sea in Israel, the Bayou Corne area in Louisiana, USA, New Mexico, and the Ebro Valley in Spain (Closson et al., 2005; Nof et al., 2013; Avni et al., 2016; Jones and Blom, 2014; Rucker et al., 2013; Gutiérrez et al., 2011). In the past three decades, time-series InSAR (Interferometric Synthetic Aperture Radar) techniques such as SBAS-InSAR and PS-InSAR have been widely applied in the field of surface settlement monitoring, enabling millimeter-scale deformation measurements over long time spans and significantly improving the capability and spatial-temporal resolution of ground deformation monitoring (Yaseen et al., 2013; Sun et al., 2023; Wang et al., 2023b; Sowter et al., 2016; Hussain et al., 2022; Ramirez et al., 2022; Nur et al., 2024; Park et al., 2024). Some studies have also successfully detected long-term precursor deformation or continuous settlement processes in major sinkhole-prone areas using InSAR, providing an important basis for early identification and risk assessment of sinkhole hazards (Chang and Hanssen, 2014).

In particular, SAR-based time-series techniques like SBAS-InSAR and PS-InSAR have demonstrated the ability to detect millimeter-scale ground movement over extended periods, providing valuable insights into gradual settlement processes that may precede sinkhole formation (Yaseen et al., 2013; Sun et al., 2023). However, these methods still face limitations when precursor signals are subtle or spatially constrained, making it difficult to distinguish abnormal patterns solely from displacement trends (Calligaris et al., 2023).

To enhance the detection of subtle precursory signals, time-frequency analysis methods such as wavelet transforms (WT) have gained attention. Wavelet analysis has proven effective for capturing localized features in non-stationary signals, including applications in seismology and climate studies (Cabieces et al., 2020; Cheng et al., 2021). By integrating continuous wavelet transform (CWT) with SBAS-InSAR, it becomes possible to identify periodic or anomalous behaviors within settlement time series.

In this study, we propose a WT-SBAS-InSAR framework to investigate the evolution of surface deformation around sinkhole-prone areas. Sentinel-1 SAR imagery was used to generate settlement time series, followed by wavelet-based multiscale decomposition to extract frequency-domain features that may indicate early signs of sinkhole development. This integrated approach aims to provide improved capabilities for early detection and risk assessment, contributing to safer urban infrastructure management.

2. STUDY AREA AND DATA COLLECTION

Sinkholes refer to sudden ground surface collapses resulting from the weakening or loss of supporting ground layers. These events can develop under natural geological conditions but are also frequently triggered by human activities such as underground excavations, leaks from deteriorating buried pipelines, or excessive groundwater extraction. In densely populated urban environments, unexpected sinkhole occurrences can cause casualties and severe damage to critical infrastructure, highlighting the urgent need for proactive monitoring and investigation of potential risk factors.

(a) Location of observation point in Yeonhui-dong

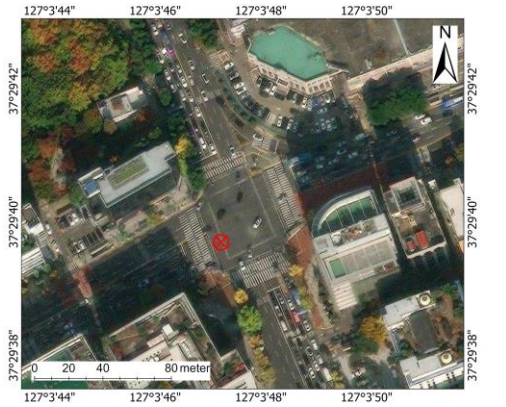

(b) Location of observation point in Gangnam-gu

Fig. 1 Overview of sinkhole sites and observation points.

In this research, two sites in Seoul that have experienced sinkhole events in the past were selected to analyze ground behavior characteristics and potential precursor signals. The selected areas—Yeonhui-dong and Gangnam-gu—are representative urban districts with complex underground structures, including subway tunnels, utility corridors, and underground commercial spaces, and they have a history of sinkhole incidents. Fig. 1 shows an overview of the study sites and the arrangement of observation points.

Yeonhui-dong is a high-density residential neighborhood in central Seoul, where localized sinkholes have appeared near public roadways, raising concerns about the stability of nearby underground facilities and urban roads. Gangnam-gu is known for its concentration of high-rise buildings, underground parking facilities, and large underground shopping malls. It has experienced sinkhole formation in commercial areas with intensive subsurface development, making continuous ground monitoring essential for urban safety.

Due to differences in local geological conditions, subsurface infrastructure layouts, and urban development patterns, these two areas provide suitable sites for comparing ground subsidence trends and detecting early warning signs of sinkhole development using satellite-based time series analysis.

For the time-series analysis of ground deformation, high-resolution satellite imagery was first used to locate and visually inspect the selected sites. Google Earth Pro was employed to identify Yeonhui-dong and Gangnam-gu as study locations. At each site, six observation points were chosen: three points situated near previous sinkhole occurrences (within approximately 5 to 20 meters) and three points positioned farther away (ranging from about 300 to over 2,000 meters). This setup allows a comparative assessment between areas directly affected by sinkholes and nearby regions with no apparent damage.

Observation points were carefully fixed based on clear surface features such as roads, buildings, and intersections identified in Google Earth Pro, ensuring consistent alignment for the time-series analysis of SAR data. This framework provided a stable spatial reference for the subsequent SBAS-InSAR processing, supporting reliable detection and comparison of ground movement patterns near sinkhole sites and their surrounding areas.

3. METHODOLOGY

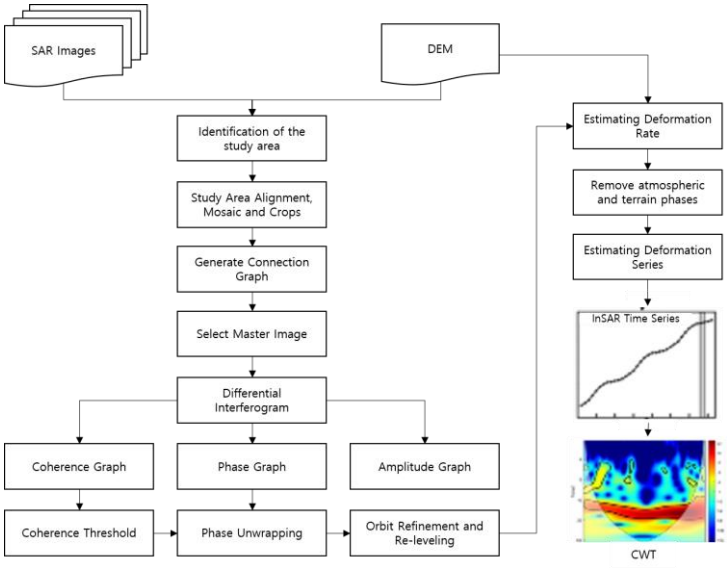

Fig. 2 Workflow

To systematically analyze the surface deformation characteristics of the sinkhole formation area, this paper designs the overall research flow as shown in Figure 2. Firstly, SBAS-InSAR technology is used to monitor the surface settlement in the study area. The specific steps include image data preprocessing, connection map construction, main image selection, interferogram generation, phase map analysis and finally inversion to obtain a continuous surface deformation time series. On this basis, the CWT (Continuous Wavelet Transform) method is further applied to the locations where sinkhole settlements have occurred to characterize the time-frequency analysis of the surface deformation, to extract the periodic change pattern of the settlement process and its scale distribution characteristics, and to provide support for the understanding of the evolution mechanism of sinkholes.

3.1 SBAS-InSAR

In order to effectively deal with the spatio-temporal incoherence issue, this study adopts the SBAS-InSAR method, which divides the existing SAR image data into several subsets by setting reasonable temporal and spatial baseline thresholds, and ensures that the spatio-temporal baselines in each subset are smaller, thus improving the coherence (Berardino et al., 2002). The method not only fully utilizes the SAR data but also maintains a high observation accuracy while reducing the solution complexity.
If $N+1$ SAR images are acquired from t_0 to t_N, the images are divided into Z short baseline subsets for the spatio-temporal baseline constraints. In each subset, the images are paired according to the short baseline criterion, and the interferograms are generated after differential interference processing. If N is specified to be an odd number, a total

of M differential interferograms are generated from Z sets of images, and M can be expressed as:

$$\frac{N+1}{2} \leq M \leq N \times \frac{N+1}{2} \tag{1}$$

where N is the number of SAR images and M is the number of differential interferograms.

Taking t_0 as the initial moment, the cumulative shape variable $d(t_i, x, r)\ t \in (i = 1, \ldots\ldots, N)$ of a certain image element (x, r) in the line-of-sight direction at t with respect to the moment of to is the quantity to be solved. If 2 SAR images at t_b and t_a (t_a is earlier than t_b) are paired to generate the kth differential interferogram, the resulting phase is $\eta\xi(t_k, x, r)\ k \in (i = 1, \ldots\ldots, M)$. Neglecting the phase error due to noise such as atmospheric effects and elevation residuals, the phase at (x, r) is

$$\eta(t_k, x, r) = \eta\xi(t_b, x, r) - \eta\xi(t_a, x, r) = \frac{4\pi[d(t_b, x, r) - d(t_a, x, r)]}{\lambda} \tag{2}$$

where $\eta\xi(t_a, x, r)$ is the image phase at moment ; $\eta\xi(t_b, x, r)$is the image phase at moment ; $d(t_a, x, r)$is the line-of-sight oriented deformation at moment t_a; $d(t_b, x, r)$ is the line-of-sight oriented deformation at moment t_b.

In actual processing, in addition to including the phase changes caused by the surface deformation, the error terms such as atmospheric delay, orbit error, elevation residuals and other noises are also inevitably superimposed. For this reason, the differential interferometric phase needs to be further modeled as an error and separated and corrected in the deformation extraction process. By establishing time-series observation equations for multiple short-baseline differential interferograms and employing inversion techniques such as the least-squares method, surface deformation information can be extracted on a continuous time series while suppressing the effect of errors.

3.2 Continuous Wavelet Transform (CWT)

To reveal the local features and periodic variation rules of signals in different time scales, this paper adopts wavelet analysis for time-frequency feature extraction. As a commonly used time-frequency localization tool, wavelet analysis can provide high resolution in both time and frequency domains at the same time, which is suitable for dealing with multi-scale variation features in non-smooth signals. In this study, continuous wavelet transform (CWT) is chosen to decompose and analyze the time series data. The continuous wavelet transform of time series variables is defined as follows(Grinsted et al., 2004):

$$W_x(\zeta, S) = \int_{-\infty}^{+\infty} x(t)\varpi^*_{\zeta,S}(t)dt \quad (3)$$

where ϖ is the subwavelet, ϖ^* is the complex conjugate, ζ is the translation parameter, and S is the scaling factor.

By convolving the signal with wavelet functions with adjustable scale and translation parameters, CWT can reveal the local energy distribution characteristics of the signal at different scales while maintaining the temporal continuity, which provides a strong support for the subsequent analysis and prevention of sinkhole deformation. Morlet wavelets were used for continuous wavelet transformation in this study. The time series sampling interval was 12 days, based on the revisit period of Sentinel-1A. The frequency band of the transform was 0.0025 to 0.0625 cycles/day.

4. RESULTS

A total of 140 Sentinel-1 images, taken at about 12-day intervals from 2018 to 2025, were used for processing. Interferometric pairs were created by linking only those images that met two baseline limits: a time gap of less than 180 days and a spatial distance within ±150 meters. This process formed a small baseline subset.

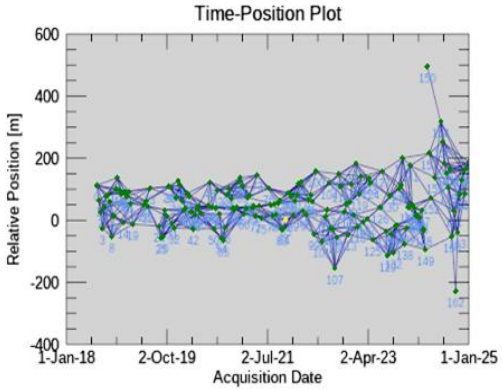

(a) Time–Position plot showing interferometric connections with no missing or disconnected scenes

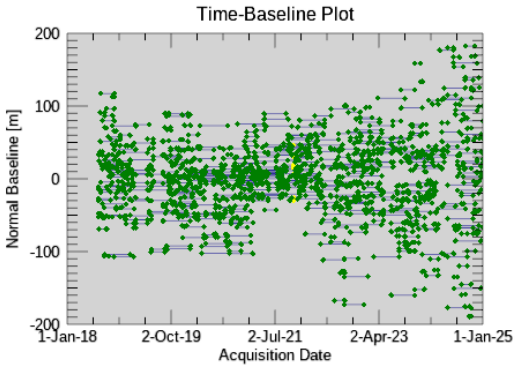

(b) Time–Baseline plot indicating all spatial baselines within ±150 m

Fig. 3 Interferometric pair selection results for SBAS-InSAR analysis.

The stability of the network was checked using a time–spatial baseline plot (Time–Position Plot, Fig. 3-a). The plot showed that all images were well connected under the set thresholds, with no missing or disconnected scenes. Each line in the plot represents one interferometric pair between a master image and a slave image. The time–baseline plot (Fig. 3-b) also confirmed that the spatial baselines stayed within ±150 meters for all images. This result showed that the image pairs were consistent and of good quality throughout the study period.

Finally, cumulative ground subsidence was calculated for each observation point, serving as the foundational dataset for subsequent Wavelet Transform analysis and the identification of anomalous settlement behavior.

4.1 Ground deformation graph

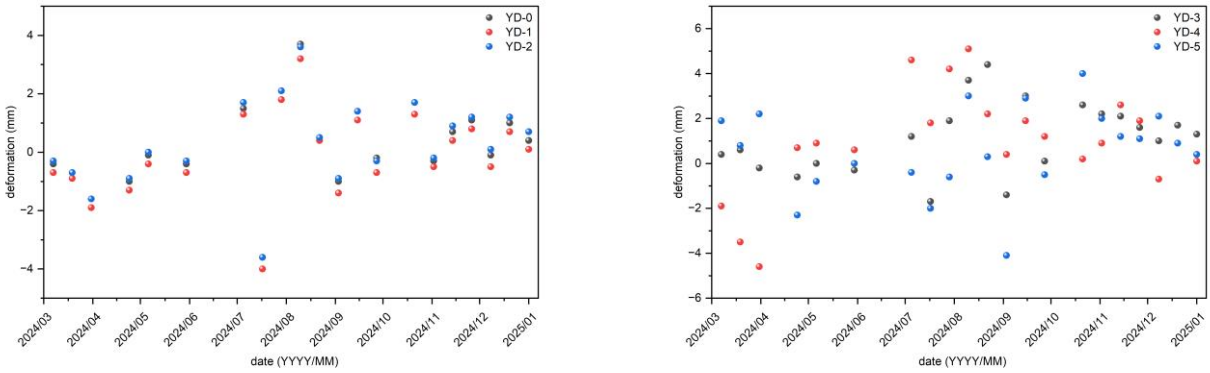

(a) Ground deformation graph near Yeonhui-dong sinkhole site

(b) Ground deformation graph at distant point from Yeonhui-dong sinkhole

Fig. 4 Ground deformation near (a) and distant from (b) Yeonhui-dong sinkhole site.

Figure 4 presents an analysis of ground displacement near the sinkhole that formed in Yeonhui-dong. The time-series data cover the period from early March 2024 through the beginning of 2025. At the sinkhole site (YD-0) and at two nearby points (YD-1 and YD-2), each located approximately 5 meters away, noticeable surface changes were detected in the period leading up to the incident. (Fig. 4-a) Specifically, the ground subsided by about 4.0 mm in mid-July and then rebounded by roughly 3.7 mm in early August, just weeks before the sinkhole event on August 29. Although these changes occurred close in time to the incident, it is still unclear whether they can be considered clear precursors. By contrast, the three more distant sites (YD-3 to YD-5), located as far as 1.3 km from the sinkhole, showed irregular displacement trends that did not align

temporally with the event. (Fig. 4-b) This suggests that any early warning signals, if present, were likely confined to the immediate area around the collapse.

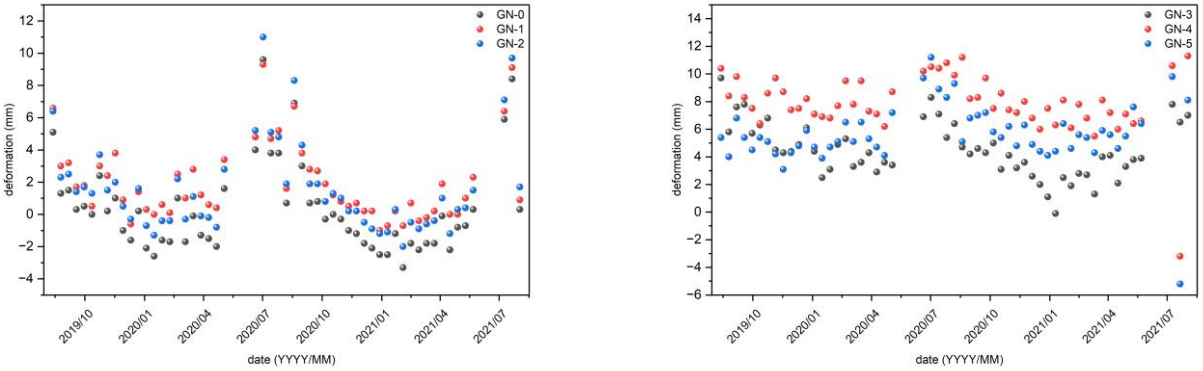

(a) Ground deformation graph near Gangnam-gu sinkhole site;

(b) Ground deformation graph at distant point from Gangnam-gu sinkhole

Fig. 5 Ground deformation near (a) and distant from (b) Gangnam-gu sinkhole site.

Figure 5 shows the subsidence patterns associated with the Gangnam-gu sinkhole, based on time-series data spanning from mid-2019 to mid-2021. The sinkhole event, which occurred in August 2020, took place during a period marked by noticeable ground movement. At the main location (GN-0) and two adjacent points (GN-1 and GN-2), a significant uplift was recorded in early July 2020, reaching a peak of approximately 11 mm. This was followed by a series of fluctuations and a gradual decline, with the lowest subsidence levels appearing in early 2021. These dynamic variations, particularly those observed between June and September 2020, coincide with the timing of the sinkhole and suggest the possibility of meaningful precursor behavior. In contrast, the distant sites (GN-3 to GN-5) exhibited similar overall displacement trends but showed no sharp changes near the event. Their patterns were more stable and gradual, indicating that the ground instability was confined to the area immediately surrounding the sinkhole.

4.2 Wavelet Transform Data

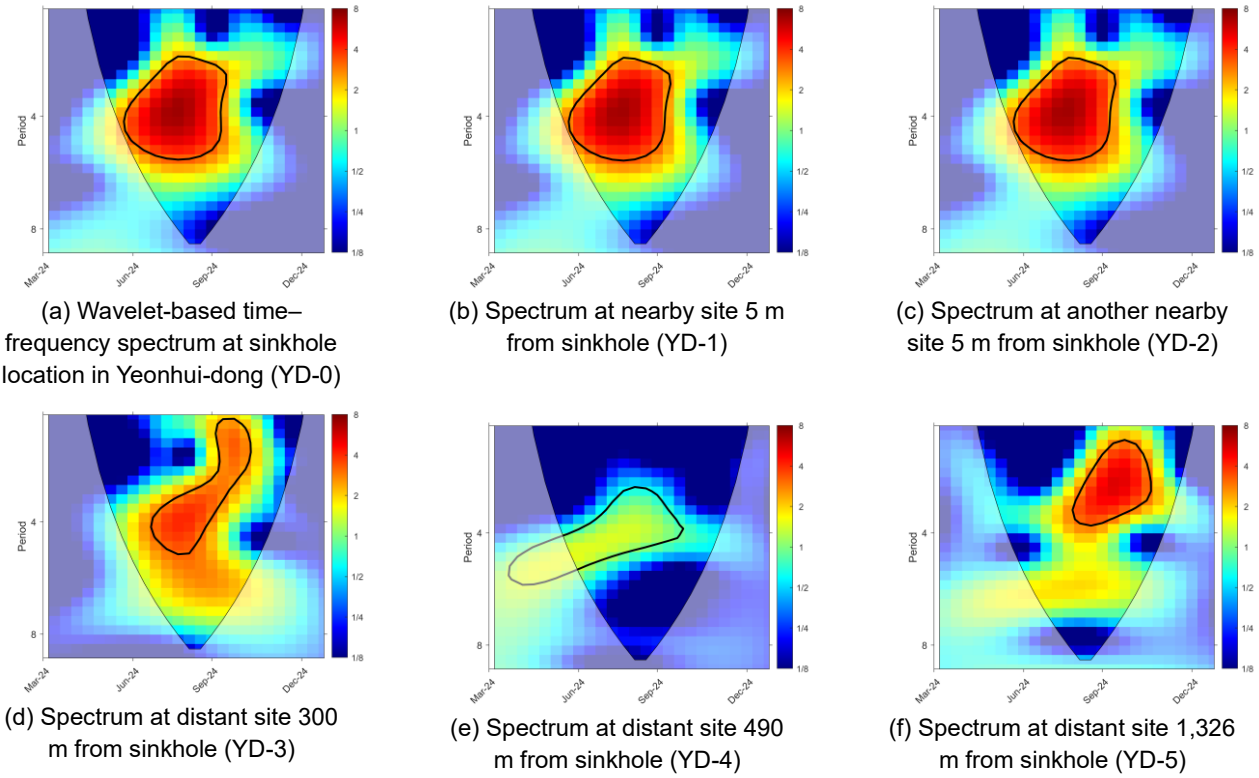

(a) Wavelet-based time–frequency spectrum at sinkhole location in Yeonhui-dong (YD-0)

(b) Spectrum at nearby site 5 m from sinkhole (YD-1)

(c) Spectrum at another nearby site 5 m from sinkhole (YD-2)

(d) Spectrum at distant site 300 m from sinkhole (YD-3)

(e) Spectrum at distant site 490 m from sinkhole (YD-4)

(f) Spectrum at distant site 1,326 m from sinkhole (YD-5)

Fig. 6 Time-series ground deformation graphs at sinkhole location and surrounding sites in Yeonhui-dong

Figure 6 presents the results of time–frequency analysis using the Wavelet Transform for the sinkhole event that occurred in Yeonhui-dong on August 29, 2024. The figure consists of six subplots, each visualizing the frequency spectrum of time-series ground displacement data collected at varying distances from the sinkhole.

Figure 6-a shows the spectrum for the sinkhole location (YD-0), while Figures 6-b and 6-c illustrate two nearby points (YD-1 and YD-2) situated approximately 5 meters away. In all three upper plots, similar high-energy responses appear within a consistent time–frequency window, with pronounced activity observed between July 5 and November 2, 2024. This period covers the sinkhole occurrence date and begins about two months in advance. The black contours visible during this interval indicate statistically significant signals, suggesting that the concentrated energy is not due to random noise but reflects meaningful anomalies.

In contrast, Figures 6-d, 6-e, and 6-f show the spectral results for more distant sites—YD-3, YD-4, and YD-5—located about 300 m, 490 m, and 1,326 m from the sinkhole, respectively. These plots reveal distinctly different patterns: the overall energy levels are lower, and the black contours appear only sporadically or are poorly defined. This indicates a weak or absent relationship between ground displacement at these distant locations and the sinkhole occurrence.

These results demonstrate that statistically significant non-stationary signals appeared in a specific frequency band near the sinkhole site before the event—signals that would

not have been identified through cumulative displacement plots alone. Conversely, the absence of such responses at greater distances highlights the spatially localized nature of the ground disturbance and the limited extent of the sinkhole's influence.

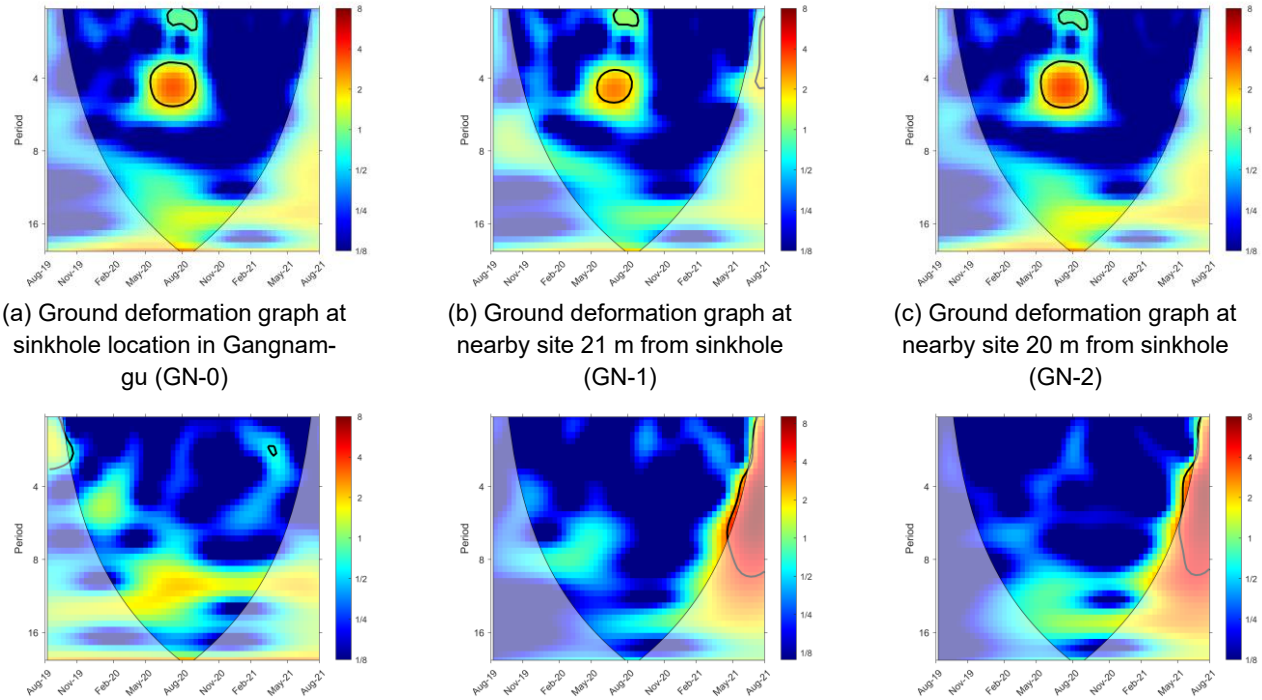

(a) Ground deformation graph at sinkhole location in Gangnam-gu (GN-0)

(b) Ground deformation graph at nearby site 21 m from sinkhole (GN-1)

(c) Ground deformation graph at nearby site 20 m from sinkhole (GN-2)

(d) Ground deformation graph at distant site 1,720 m from sinkhole (GN-3)

(e) Ground deformation graph at distant site 1,053 m from sinkhole (GN-4)

(f) Ground deformation graph at distant site 1,100 m from sinkhole (GN-5)

Fig. 7 Time-series ground deformation graphs at sinkhole location and surrounding sites in Gangnam-gu

Figure 7 presents the results of Wavelet Transform analysis applied to the sinkhole event that occurred in Gangnam-gu on August 3, 2020. Figures 7-a, 7-b, and 7-c (upper row) show the spectral results for the sinkhole location (GN-0) and two adjacent sites located 21 m (GN-1) and 20 m (GN-2) away, respectively. Figures 7-d, 7-e, and 7-f (lower row) display the results for more distant sites located 1,720 m (GN-3), 1,053 m (GN-4), and 1,100 m (GN-5) from the sinkhole.

At all three adjacent sites, a clear high-energy response was observed from May 3 to October 6, 2020. Statistically significant anomalous signals appeared within similar time and frequency bands, indicated by black contours. This interval begins approximately three months before the sinkhole event. The signal shown in Figure 7-a was especially notable, featuring both high intensity and a broad area of influence, suggesting its potential as an early warning sign.

In contrast, the distant sites exhibited generally weak frequency responses. Even when black contours were present, they appeared sporadically and lacked consistent timing or

frequency structure. The power spectra at these locations mostly displayed stable, low-energy distributions, typically shown in blue.

The Gangnam case once again demonstrates that Wavelet Transform analysis is effective for detecting early-stage, short-term ground anomalies. The early emergence of anomalous signals and the consistent frequency response patterns across the sinkhole site and its adjacent areas highlight the method's value in identifying precursory ground deformation.

This study applied a time–frequency analysis approach using the Wavelet Transform to time-series ground displacement data obtained through the SBAS-InSAR technique, with the objective of exploring how surface deformation patterns relate to sinkhole formation. The analysis showed that, at locations where sinkholes were reported, there was a distinct rise in energy within a certain high-frequency band (corresponding to periods between 4 and 8) starting several months before the sinkhole event. Such anomalous signals could not be captured through cumulative subsidence curves alone, indicating that these patterns may serve as potential early warning signs. By contrast, at sites farther away within the same areas, no comparable frequency responses were detected, supporting the conclusion that these ground failure signals are spatially localized.

Overall, these findings illustrate the shortcomings of relying solely on traditional time-domain monitoring and highlight the benefit of adding frequency-domain anomaly detection to enhance the accuracy and timeliness of hazard prediction. The WT-SBAS-InSAR method developed in this research suggests a practical and robust framework that can be applied to urban ground stability assessments, sinkhole hazard forecasting, and the advancement of early warning systems.

5. ANALYSIS

In this study, the WT-SBAS-InSAR approach was applied using Sentinel-1 SAR data to analyze two sinkhole-prone areas in Seoul Metropolitan City: Yeonhui-dong and Gangnam-gu. This framework combines cumulative ground subsidence estimation using SBAS-InSAR with a time–frequency analysis based on the Wavelet Transform, allowing both long-term trends and cyclic characteristics of ground deformation to be examined simultaneously. For each study area, the ground behavior was investigated by distinguishing between locations adjacent to sinkholes and distant reference sites, providing a more quantitative understanding of precursor patterns beyond simple cumulative subsidence observations.

The cumulative settlement profiles derived from the SBAS-InSAR technique showed that displacement tended to increase from the point of sinkhole occurrence at nearby sites, but this trend was often gradual and sometimes unclear. Especially in areas where the total amount of settlement was relatively small or progressed slowly, it was challenging to identify clear precursors solely from cumulative displacement data.

To address this limitation, the same time-series data were analyzed further using the Wavelet Transform, which extracts signal characteristics in the time–frequency domain.

This analysis revealed that near the actual sinkhole sites, a marked increase in energy appeared in a specific high-frequency range (corresponding to periods between 4 and 8) around the time of the event. Such high-frequency responses may reflect structural heterogeneity and stress concentration within the ground. In contrast, the distant reference sites in the same areas maintained stable energy distributions throughout the analysis period, and no comparable anomalies were found.

These results demonstrate that the WT-SBAS-InSAR framework can effectively capture both long-term subsidence patterns and localized, transient anomalies in ground deformation at sinkhole-susceptible locations. The ability to isolate energy concentrations within specific time scales makes it possible to detect subtle deformation signals that could act as early indicators of sudden surface collapse. This highlights the potential of wavelet-based analysis as a valuable tool for urban geohazard early warning systems and predictive ground stability models.

While this approach shows promise, applying it to larger or more densely built-up urban environments presents several challenges. As the spatial coverage expands, the computational burden of processing high-resolution time-series data increases substantially. Moreover, variations in surface conditions such as vegetation cover, ongoing construction, or land use can lower coherence and affect the reliability of time–frequency decomposition results. Additionally, current workflows often rely on manual interpretation of localized wavelet energy patterns; future research should focus on integrating automated anomaly detection and classification algorithms to enhance scalability and practical application. Addressing these issues will be critical for broader adoption of this technique in urban infrastructure monitoring systems.

6. CONCLUSIONS

The WT-SBAS-InSAR approach was applied to four sinkhole-prone areas in Seoul — Yeonhui-dong and Gangnam-gu— using Sentinel-1 Synthetic Aperture Radar (SAR) data. This integrated method combines two analytical steps: a time-series displacement analysis based on the Small Baseline Subset Interferometric SAR (SBAS-InSAR) and a frequency-domain evaluation through wavelet transform. The aim was to simultaneously capture both long-term settlement patterns and short-term irregular changes in ground behavior.

For each observation point, cumulative displacement graphs were produced to visualize overall trends, which were particularly informative near the sinkhole sites. In many cases, these graphs revealed a gradual increase in ground movement following the sinkhole occurrence date. However, when the amount of displacement was small or developed slowly, cumulative trends alone were not sufficient to identify early warning signs before the event.

To address this gap, the same time-series data were further analyzed using wavelet transform, which tracks how signal energy varies across both time and frequency. This revealed that, at locations where sinkholes formed, a notable surge in energy appeared in a specific frequency band — corresponding to levels 4 to 8 — around the time of occurrence. This type of response likely reflects stress concentration or local

heterogeneity within the ground. In contrast, other nearby sites that did not experience sinkholes displayed stable energy patterns and did not exhibit any significant anomalies.

These findings demonstrate that small but critical precursory signals may be overlooked if ground monitoring relies only on cumulative settlement data. By adding wavelet-based frequency analysis, subtle early-stage indicators can be detected that might otherwise remain hidden. The results show that combining both methods provides a more comprehensive understanding of ground behavior, making it more practical for identifying potential risks before a sinkhole develops.

Overall, relying on positional cumulative graphs alone is not sufficient for pinpointing local subsidence or emerging sinkhole threats in dense urban areas. Detecting such risks requires examining cyclic patterns and abrupt changes in signal behavior alongside traditional trend analysis. The WT-SBAS-InSAR framework can be widely applied to urban ground stability monitoring, development of predictive geohazard models, and implementation of smart early warning systems. As such, this combined approach offers a valuable foundation for protecting urban infrastructure and mitigating the impacts of ground-related hazards.

ACKNOWLEDGEMENTS

This work was supported by the National Research Foundation of Korea (NRF) grant funded by the Korea government (MSIT) (No. RS-2021-NR060085).

REFERENCES

Berardino, P., Fornaro, G., Lanari, R. and Sansosti, E. (2002), “A new algorithm for surface deformation monitoring based on small baseline differential SAR interferograms,” IEEE Trans. Geosci. Remote Sens., **40**, 2375-2383.

Cabieces, R., Krüger, F., Garcia-Yeguas, A., Villaseñor, A., Buforn, E., Pazos, A., Olivar-Castaño, A. and Barco, J. (2020), “Slowness vector estimation over large-aperture sparse arrays with the Continuous Wavelet Transform (CWT): Application to Ocean Bottom Seismometers,” Geophys. J. Int., **223**, 1919-1934.

Calligaris, C., Forte, E., Busetti, A. and Zini, L. (2023), “A joint geophysical approach to tune an integrated sinkhole monitoring method in evaporitic environments,” Near Surf. Geophys., **21**, 317-332.

Carbonel, D., Rodríguez, V., Gutiérrez, F., McCalpin, J.P., Linares, R., Roqué, C., Zarroca, M., Guerrero, J. and Sasowsky, I. (2014), “Evaluation of trenching, ground penetrating radar (GPR) and electrical resistivity tomography (ERT) for sinkhole characterization,” Earth Surf. Process. Landforms, **39**, 214-227.

Chang, L. and Hanssen, R.F. (2014), “Detection of cavity migration and sinkhole risk using radar interferometric time series,” Remote Sens. Environ., **147**, 56-64.

Dobecki, T.L. and Upchurch, S.B. (2006), “Geophysical applications to detect sinkholes and ground subsidence,” Leading Edge, **25**, 336-341.

Engelbrecht, J., Inggs, M.R. and Makusha, G. (2011), "Detection and monitoring of surface subsidence associated with mining activities in the Witbank Coalfields, South Africa, using differential radar interferometry," S. Afr. J. Geol., **114**, 77-94.

Gutiérrez, F., Galve, J.P., Lucha, P., Castañeda, C., Bonachea, J. and Guerrero, J. (2011), "Integrating geomorphological mapping, trenching, InSAR and GPR for the identification and characterization of sinkholes: A review and application in the mantled evaporite karst of the Ebro Valley (NE Spain)," Geomorphology, **134**, 144-156.

Gutiérrez, F., Parise, M., De Waele, J. and Jourde, H. (2014), "A review on natural and human-induced geohazards and impacts in karst," Earth-Sci. Rev., **138**, 61-88.

Jones, C.E. and Blom, R.G. (2014), "Bayou Corne, Louisiana, sinkhole: Precursory deformation measured by radar interferometry," Geology, **42**, 111-114.

Kaufmann, O. and Quinif, Y. (2002), "Geohazard map of cover-collapse sinkholes in the 'Tournaisis' area, southern Belgium," Eng. Geol., **65**, 117-124.

Nof, R.N., Baer, G., Ziv, A., Raz, E., Atzori, S. and Salvi, S. (2013), "Sinkhole precursors along the Dead Sea, Israel, revealed by SAR interferometry," Geology, **41**, 1019-1022.

Sowter, A., Amat, M.B.C., Cigna, F., Marsh, S., Athab, A. and Alshammari, L. (2016), "Mexico City land subsidence in 2014–2015 with Sentinel-1 IW TOPS: Results using the Intermittent SBAS (ISBAS) technique," Int. J. Appl. Earth Obs. Geoinf., **52**, 230-242.

Sun, H., Peng, H., Zeng, M., Wang, S., Pan, Y., Pi, P., Xue, Z., Zhao, X., Zhang, A. and Liu, F. (2023), "Land subsidence in a coastal city based on SBAS-InSAR monitoring: A case study of Zhuhai, China," Remote Sens., **15**, 2424.

Theron, A. and Engelbrecht, J. (2018), "The role of earth observation, with a focus on SAR interferometry, for sinkhole hazard assessment," Remote Sens., **10**, 1506.

Van Den Eeckhaut, M., Poesen, J., Dusar, M., Martens, V. and Duchateau, P. (2007), "Sinkhole formation above underground limestone quarries: A case study in South Limburg (Belgium)," Geomorphology, **91**, 19-37.

Weary, D.J. (2015), "The cost of karst subsidence and sinkhole collapse in the United States compared with other natural hazards,", U.S. Geological Survey.

Yaseen, M., Hamm, N.A., Woldai, T., Tolpekin, V.A. and Stein, A. (2013), "Local interpolation of coseismic displacements measured by InSAR," Int. J. Appl. Earth Obs. Geoinf., **23**, 1-17.